NATIONAL ADVISORY COMMITTEE FOR AERONAUTICS

TECHNICAL NOTE 2834

FLOW SURFACES IN ROTATING AXIAL-FLOW PASSAGES

By John D. Stanitz and Gaylord O. Ellis

Lewis Flight Propulsion Laboratory
Cleveland, Ohio

NACA

Washington
November 1952

1H

NATIONAL ADVISORY COMMITTEE FOR AERONAUTICS

TECHNICAL NOTE 2834

FLOW SURFACES IN ROTATING AXIAL-FLOW PASSAGES

By John D. Stanitz and Gaylord O. Ellis

2617

SUMMARY

In order to investigate the deviation of flow surfaces from their assumed orientation in the usual type of two-dimensional solution, three-dimensional, incompressible, nonviscous, absolute irrotational fluid motion is determined for flow through rotating axial-flow passages bounded by straight blades of finite spacing and infinite axial length lying on meridional planes. Solutions are obtained for five passages with varying blade spacing and hub-tip ratio. The results are presented in such a manner as to apply for all ratios of axial velocity to passage tip speed. It is concluded that, for conditions in typical axial-flow blade rows, the deviation of flow surfaces from their assumed orientation in two-dimensional solutions is small.

INTRODUCTION

A flow surface in the passage between two blades of a compressor or turbine is generated by the motion through the passage of any fluid line consisting of the same fluid particles and extending from one boundary to another in a plane normal to the axis of rotation. In two-dimensional analyses of flow in compressors and turbines, the fluid motion is usually assumed to occur on flow surfaces that are: (1) surfaces of revolution about the axis of the turbomachine (blade-to-blade solutions, references 1 and 2, for example) or (2) mean passage surfaces that are congruent with the mean blade surfaces (hub-to-shroud solutions, references 3 and 4, for example). Actually, the flow surfaces deviate from the orientation assumed for the two-dimensional solutions and, in the direction of flow, become progressively more tilted and distorted. This deviation of the flow surfaces from their assumed orientation is caused by spanwise variations of blade loading and, in rotating blade rows, by rotation of the fluid particles relative to the passage in a plane normal to the axis of the blade row. This rotation is required to maintain the rotational or irrotational character of the absolute fluid motion.

The deviation of flow surfaces is considered in reference 5, but no attempt is made to estimate the magnitude of this phenomenon. An analytical investigation has therefore been made at the NACA Lewis laboratory in order to determine the magnitude of this deviation in rotating axial-flow passages. The axial-flow passages in this investigation are bounded by straight blades of finite spacing and infinite axial length lying on meridional (axial-radial) planes. The solutions have been made for three-dimensional, incompressible, nonviscous, absolute irrotational fluid motion over a range of blade spacings and hub-tip ratios. These solutions do not investigate the effect of spanwise distribution of blade loading, which was considered of secondary importance. (Note that, as in rectangular elbows with potential flow, uniform spanwise loading has no effect on the deviation of flow surfaces.) Likewise, the effects of compressibility have not been investigated because, as clearly indicated by the correlation equations in reference 1, the eddy flow, which causes the flow surfaces to deviate, is little affected by compressibility. The results are presented in such a manner as to apply to any ratio of blade-tip speed to axial velocity of the fluid.

METHOD OF SOLUTION

The method of solution, including the relaxation solution of the differential equation of flow and the superposition of solutions, is developed in this section.

Preliminary Considerations

Assumptions. - The absolute flow is assumed to be irrotational. The fluid is assumed to be nonviscous and incompressible. The fluid motion is three dimensional and is steady relative to the rotating passage.

Coordinate system and velocity components. - The cylindrical coordinate system r, θ, z is shown in figure 1. (All symbols are defined in appendix A). The linear coordinates r and z are expressed as ratios of the blade-tip radius. Thus, for example, the radius r at the blade tip is unity. The coordinate system is fixed relative to the passage which rotates about the z-axis in the positive direction according to the right-hand rule.

The velocity components u, v, w relative to the coordinate system in the r, θ, z directions, respectively, are also shown in figure 1. The velocity components and the blade speed are expressed as ratios of the blade-tip speed. Thus, for example, the blade speed at any radius is equal to r and the absolute tangential velocity component becomes $(v + r)$.

Type of passage geometry. - The rotating axial-flow passages in this investigation are infinitely long. Each passage is bounded by a hub and casing of constant radius, respectively, and by straight blades of finite spacing and infinite length lying on meridional (axial-radial) planes. The blade inlet is considered to be at minus infinity in the z-direction and the blade exit at plus infinity. Under these circumstances the flow is uniform in the z-direction at the region investigated (near the origin, z = 0) and the blade loading is zero. Thus, effects of blade loading on deviation of the flow surfaces are not investigated in this report. These effects are considered of secondary importance.

Superposition of solutions. - For the passage geometry just described, the incompressible flow solution can be separated into two parts: (1) the rotating or eddy-flow solution in the rotating passage with no through flow and (2) the through-flow solution in the stationary passage with no eddy flow. The eddy-flow solution does not change in the z-direction and is therefore two dimensional. The through-flow solution is a uniform axial velocity w. Various percentages of the two solutions can be combined by linear superposition to obtain new solutions for different ratios of axial velocity to blade-tip speed, that is, for different values of w.

Eddy-Flow Solution

The eddy-flow solution is two dimensional and lies in the $r\theta$-plane.

Continuity. - A fluid particle on the $r\theta$-plane is shown in figure 2. From continuity considerations

$$\frac{\partial}{\partial r}(ru) + \frac{\partial v}{\partial \theta} = 0 \tag{1}$$

A stream function ψ satisfies equation (1) if defined as

$$\frac{\partial \psi}{\partial \theta} = ru \tag{2a}$$

$$\frac{\partial \psi}{\partial r} = -v \tag{2b}$$

Irrotational absolute motion. - For irrotational absolute motion, the circulation of the absolute velocity around the fluid particle in figure 2 is zero, and therefore

$$\frac{\partial}{\partial r}\left[(r + v)r\right] - \frac{\partial u}{\partial \theta} = 0$$

or

$$\frac{\partial v}{\partial r} + \frac{v}{r} - \frac{1}{r}\frac{\partial u}{\partial \theta} = -2 \tag{3a}$$

which, after substitution of equation (2), becomes

$$\frac{\partial^2 \psi}{\partial r^2} + \frac{1}{r}\frac{\partial \psi}{\partial r} + \frac{1}{r^2}\frac{\partial^2 \psi}{\partial \theta^2} = 2 \tag{3b}$$

Equation (3b) is the differential equation of flow that determines the distribution of ψ for the eddy-flow solution in the $r\theta$-plane.

Transformation of coordinates. - In order to solve equation (3) by relaxation methods, it is convenient to transform the $r\theta$-plane onto the $\xi\theta$-plane by means of

$$\xi = \ln r \tag{4}$$

from which equation (3b) becomes

$$\frac{\partial^2 \psi}{\partial \xi^2} + \frac{\partial^2 \psi}{\partial \theta^2} = 2r^2 \tag{5}$$

Relaxation solution. - Equation (5) is solved by relaxation methods (references 6 and 7, for example) to satisfy the specified boundary conditions. For the eddy-flow solutions, there is no flow through the passage so that ψ is zero along the hub, shroud, and blade surfaces. In the $\xi\theta$-plane these boundaries form a rectangle within which is placed a grid of equally spaced points. At each of these grid points the value of ψ required to satisfy equation (5) in finite difference form is determined by relaxation methods. The size of the grid spacing varies among examples and will be indicated later. The values of ψ at the grid points were relaxed to a unit change in the fifth decimal. The velocity components are obtained from the distribution of ψ according to equation (2). The streamlines of the eddy flow in the $r\theta$-plane are lines of constant ψ.

Combined Solutions

For the eddy-flow solutions on the $r\theta$-plane, the fluid rotates relative to the passage walls in a direction opposite to that of the blade rotation. This fluid motion is the same for all planes normal to the z-axis. For the through-flow solution the axial velocity w is everywhere constant. These two linear solutions can be superposed to obtain solutions for three-dimensional flow through rotating axial-flow passages.

It is desired to determine the flow surface generated by the motion of any fluid line that extends between boundaries in the $r\theta$-plane and always consists of the same fluid particles. This fluid line rotates with the fluid in the $r\theta$-plane and the surface that it generates depends on the velocity w with which it moves in the axial direction through the passage. Examples of such flow surfaces are shown in figure 3. The shape of these surfaces can be indicated on the $r\theta$-plane alone by plots of the intersections of these surfaces with the $r\theta$-plane at equal increments of z. These intersections are the positions of the fluid lines on the $r\theta$-planes at these values of z. If, instead of increments of z, however, fluid lines are plotted on the $r\theta$-plane for increments of the absolute angle α that the passage has rotated about the z-axis, these fluid-line positions apply for all values of w. For a given value of α, the value of z then depends on w and this relation is given by

$$z = \alpha w \tag{6}$$

Thus the results of the combined solutions are plotted as fluid-line positions in the $r\theta$-plane for equal increments of α and these results (fig. 4(a), for example) apply for all ratios w of through-flow velocity to blade-tip speed. The three-dimensional flow surfaces in figure 3 correspond to the fluid-line positions shown in figure 4(a) for w equal to 0.6.

NUMERICAL EXAMPLES

The results for three-dimensional flow through five rotating axial-flow passages are presented in figures 4 to 8. The results are presented in the $r\theta$-plane by streamlines ψ^* of the eddy-flow solution and by fluid-line positions α of the three-dimensional flow surfaces. The streamlines are designated by ψ^*, which is defined as

$$\psi^* = \frac{\psi}{\psi_{min}} \tag{7}$$

where the subscript min refers to the algebraic minimum value of ψ so that ψ^* varies from zero along the boundaries to 1.0 at the point of minimum ψ. The fluid-line positions in the $r\theta$-plane are indicated for various values of the absolute angle α that the passage has rotated about the z-axis from its initial position ($\alpha = 0$) at which the fluid-line positions are radial or circumferential lines. In conformity with reference 5, flow surfaces with initial fluid-line positions that are circumferential or radial lines are designated S_1- or S_2-surfaces, respectively.

Passage configurations. - The geometry of the five axial-flow passages investigated is described in table I.

TABLE I - GEOMETRY OF AXIAL-FLOW PASSAGES

Example	Hub-tip ratio r_h	Blade spacing $\Delta\theta$		Grid spacing
		radians	deg	
I(standard)	0.70000	0.17834	10°13'	$(\Delta\theta/8)$ = 0.02229
II	.70000	.08917	5° 7'	$(\Delta\theta/8)$ = .01115
III	.70000	.35667	20°26'	$(\Delta\theta/8)$ = .04458
IV	.50105	.17834	10°13'	$(\Delta\theta/8)$ = .02229
V	.89453	.17834	10°13'	$(\Delta\theta/16)$= .01115

2617

The results of the standard solution, example I, are compared with the results of examples II and III to determine the effect of varying the blade spacing $\Delta\theta$ with constant hub-tip ratio r_h. The results of example I are also compared with examples IV and V to determine the effect of varying r_h with $\Delta\theta$ constant. The grid spacings used in the relaxation solutions are given in the last column of the table.

Standard solution. - Results for the standard solution (example I) are presented in figure 4. In figure 4(a) are shown fluid-line positions of the central flow surfaces for various values of the angle α. The central flow surfaces are defined as those surfaces for which the fluid lines pass through the point of minimum ψ, that is, $\psi^* = 1.0$. At this point, values of u and v are both zero so that the central flow surfaces pivot about a straight line in the z-direction through this point.

In figure 4(b) are shown the fluid-line positions of off-center S_1-surfaces for various values of the angle α. For any off-center flow surface, the envelope of the fluid-line positions for various values of α is a streamline. This fact is clearly shown by the upper S_1-surface in figure 4(b) which is tangent to the streamline 0.8.

Fluid-line positions of off-center S_2-surfaces for various values of α are shown in figure 4(c). Finally, in figure 4(d), are shown fluid-line positions of the central S_1-surface for a wide range of α. As α increases, the surface becomes progressively more distorted because its velocity in the $r\theta$-plane along the boundaries near the corners is low, becoming equal to zero at the corners, whereas the velocities along most of the other eddy-flow streamlines approach a wheel-type distribution with zero velocity at $\psi^* = 1.0$. It is concluded that, for large values of the absolute angle α, the flow surfaces become greatly distorted.

Solutions for effect of blade spacing. - Examples II and III are presented in figures 5 and 6. These figures, together with figure 4(a), indicate the shapes of the central flow surfaces for three blade spacings $\Delta\theta$ with the same hub-tip ratio r_h. The general appearance of the central S_1-surfaces is similar for examples I and II, and in example III the S_1- and S_2-surfaces are similar. Reasons for these similarities are given in DISCUSSION OF RESULTS.

Solutions for effect of hub-tip ratio. - Examples IV and V are presented in figures 7 and 8. These figures, together with figure 4(a), indicate the shapes of the central flow surfaces for three hub-tip ratios r_h with the same blade spacing $\Delta\theta$. The general appearance of the central S_1-surfaces of examples I and IV is similar, and the S_1- and S_2-surfaces of example V are similar to the S_2- and S_1-surfaces, respectively, of example I. Also, it is noted that the central S_1- and S_2-surfaces of examples II and IV are similar in general appearance. Reasons for these similarities are given in DISCUSSION OF RESULTS.

DISCUSSION OF RESULTS

Some of the results presented in figures 4 to 8 are discussed, and the deviations of the flow surfaces from their initial positions for α equal to zero in the $r\theta$-plane are investigated.

Typical value for α. - The results in figures 4 to 8 are presented as fluid-line positions in the $r\theta$-plane for even increments of α. As already defined, α is the absolute angle that the axial-flow passage has rotated about the z-axis, with α equal to zero when the initial position of the fluid line is a circumferential line (S_1-surface) or radial line (S_2-surface) in the $r\theta$-plane. This angle α is related to the geometry and operating conditions of the axial-flow passage by equation (6). In order to determine a typical value for α, an axial-flow stage is considered with

$$w' = 550 \text{ ft/sec}$$

$$z' = 0.12 \text{ ft } (1.44 \text{ in.})$$

$$\omega' = 838 \text{ radians/sec } (8000 \text{ rpm})$$

where the prime superscript indicates dimensional quantities. Equation (6) becomes

$$\alpha = \frac{z'\omega'}{w'} = 0.183$$

so that a typical value for α is approximately 0.2. From figures 4 to 8 it is therefore concluded that the deviation of flow surfaces in typical axial-flow blade rows is not large. This conclusion is further strengthened if the fluid-line position for α equal to zero is considered to occur halfway through the blade row. Then the maximum deviation of the surface from its position at α equal to zero is reduced by approximately one half.

For blade rows (not necessarily axial flow) with relatively large dimensions in the direction of flow, such as radial- and mixed-flow impellers, the deviations of the flow surfaces must be large. However, even these large deviations do not invalidate the two-dimensional solutions completely, because, as shown in reference 8, at many positions in the passage the velocity components of major importance are much the same for two- and three-dimensional solutions.

Deviation of flow surfaces. - The deviation of flow surfaces from their initial orientation, given by fluid-line positions in the $r\theta$-plane at α equal zero, can be described by three factors (fig. 9): (1) displacement, in the $r\theta$-plane, of the tangent point between the fluid line and the tangent streamline; (2) rotation, in the $r\theta$-plane, of the fluid line about this tangent point; and (3) distortion or bending of the fluid line in the $r\theta$-plane. The displacement of the tangent point is determined by its motion in the $r\theta$-plane along the streamline with which the fluid line is tangent. This displacement for off-center S_1- and S_2-surfaces is indicated in figures 4(b), 4(c), and 9 and will not be discussed further. For central flow surfaces, which will be considered exclusively hereinafter, the tangent point (center point) does not move and the displacement is zero.

The rotation of central flow surfaces will be measured by the angle $\beta - \beta_0$ which the tangent to the fluid line at its center point rotates in the $r\theta$-plane from its initial position β_0 at α equals zero (fig. 9). The angle β is measured clockwise from the radial direction so that β_0 is 90° for S_1-surfaces and 0° for S_2-surfaces.

The distortion of the flow surfaces will be discussed qualitatively.

Rotation of flow surfaces. - The rotation of central flow surfaces is measured by the angle $\beta - \beta_0$ introduced in the preceding section. This angle can be measured in figures 4(a) and 5 to 8. However, an equation has been developed (appendix B) by which the rotation $\beta - \beta_0$ can be determined directly from α and a parameter A, which is the value of $\frac{\partial^2 \psi}{\partial r^2}$ at the center point.

For central S_1-surfaces

$$\tan(\beta - \beta_0)_1 = -\sqrt{\frac{2 - A}{A}} \tan\left[\alpha \sqrt{A(2 - A)}\right] \tag{7a}$$

and for central S_2-surfaces

$$\tan(\beta - \beta_0)_2 = -\sqrt{\frac{A}{2 - A}} \tan\left[\alpha \sqrt{A(2 - A)}\right] \tag{7b}$$

so that the rotations of the two types of central flow surface are related by

$$\tan(\beta - \beta_0)_1 = \left(\frac{2 - A}{A}\right) \tan(\beta - \beta_0)_2 \tag{7c}$$

In particular, for A equal to 1.0,

$$(\beta - \beta_0)_1 = (\beta - \beta_0)_2 = \alpha \tag{7d}$$

so that the rotation of both flow surfaces are equal to the rotation α of the passage about the z-axis.

As will be discussed later in this section, the parameter A is primarily a function of $\frac{\ln r_h}{\Delta\theta}$. If $\frac{\ln r_h}{\Delta\theta}$ is zero, that is, if r_h is 1.0 and $\Delta\theta$ is finite, v and $\frac{\partial u}{\partial \theta}$ are zero at the center point and equation (3a) gives

$$\frac{\partial v}{\partial r} = -2$$

from which

$$A = \frac{\partial^2 \psi}{\partial r^2} = -\frac{\partial v}{\partial r} = 2$$

Also, if $\frac{\ln r_h}{\Delta\theta}$ is infinite, that is, if $\Delta\theta$ is zero and r_h is less than 1.0, $\frac{\partial v}{\partial r}$ is zero at the center point so that

$$A = \frac{\partial^2 \psi}{\partial r^2} = -\frac{\partial v}{\partial r} = 0$$

Thus, the parameter A varies between 0 and 2.0 as $\frac{\ln r_h}{\Delta\theta}$ varies between $-\infty$ and 0. For A equal to 0, equations (7a) and (7b) become

$$\tan(\beta - \beta_0)_1 = -2\alpha \tag{7e}$$

and

$$\tan(\beta - \beta_0)_2 = 0 \tag{7f}$$

Likewise, for A equal to 2.0, equations (7a) and (7b) become

$$\tan(\beta - \beta_0)_1 = 0 \tag{7g}$$

and

$$\tan(\beta - \beta_0)_2 = -2\alpha \tag{7h}$$

The rotation $(\beta - \beta_0)_1$ of central S_1-surfaces has been computed by equations (7a), (7e), and (7g) and is plotted in figure 10 as a function of α for various values of A. The rotation $(\beta - \beta_0)_2$ of central S_2-surfaces is also given by figure 10 if the curves of constant A are numbered in reverse order. Thus, discussions relating to the rotation of central S_1-surfaces with parameter A equal to x also apply to the rotation of central S_2-surfaces with A equal to (2 - x).

In figure 10 the curve for A equal to zero is asymptotic to $\pi/2$, or 1.5708. For this value of A, the passage width is zero ($\Delta\theta = 0$), and the central S_1-surface cannot rotate more than $\pi/2$ radians. For A equal to 2.0, the rotation $(\beta - \beta_0)_1$ is zero at all values of α. For this value of A, the passage height is zero ($r_h = 1.0$), and the central S_1-surface cannot rotate. As indicated by equation (7d), a linear relation exists between $(\beta - \beta_0)_1$ and α for A equal to 1.0. As will be shown later in this section, for this value of A the average passage width is approximately equal to the passage height (example III, fig. 6), and both the central S_1- and S_2-surfaces rotate at the same rate as the passage itself, but in the opposite direction. For the remaining values of A, the curves in figure 10 have inflection points at $(\beta - \beta_0)_1$ equal to $\pi/2$, π, and so forth. For values of A less than 1.0, the rate of change of $(\beta - \beta_0)_1$ with α is minimum at $(\beta - \beta_0)_1$ equal to $\frac{\pi}{2}$, $3\frac{\pi}{2}$, and so forth, and is maximum at $(\beta - \beta_0)_1$ equal to π, 2π, and so forth. For values of A greater than 1.0, the reverse is true. In all cases, the rate of change of $(\beta - \beta_0)_1$ with α is greatest when the tangent to the fluid line at its center point is oriented in the direction of minimum distance between passage walls and is least when the tangent is oriented normal to the direction of minimum distance. This observation is reasonable because, as indicated by the streamline spacing for examples I to V, the gradient of the velocity

component normal to the tangent of the fluid line at its center point, which velocity gradient causes the fluid line to rotate about its center point, is maximum when the tangent is oriented in the direction of minimum distance between passage walls and is minimum when the tangent is oriented normal to the direction of minimum distance.

The parameter A, which determines the rotation of the central flow surfaces, is primarily a function of the ratio $\frac{\ln r_h}{\Delta\theta}$. The values of A for examples I to V have been obtained from the relaxation solutions and are given in table II together with the values of

TABLE II - VALUES OF PARAMETER A

Example	A	$\frac{\ln r_h}{\Delta\theta}$
I	0.314	-2
II	.134	-4
III	1.020	-1
IV	.240	$-3\frac{7}{8}$
V	1.535	$-\frac{5}{8}$

$\frac{\ln r_h}{\Delta\theta}$. These values of A and $\frac{\ln r_h}{\Delta\theta}$ are plotted in figure 11. As previously discussed, the parameter A is equal to 2 and zero for $\frac{\ln r_h}{\Delta\theta}$ equal to zero and $-\infty$, respectively. It can be shown analytically that the curve in figure 11 has zero slope for $\frac{\ln r_h}{\Delta\theta}$ equal to zero. As $\frac{\ln r_h}{\Delta\theta}$ varies from zero to $-\infty$, the passage geometry in the $r\theta$-plane varies from a wide shape with zero height in the r-direction to a tall shape with zero width in the θ-direction. For $\frac{\ln r_h}{\Delta\theta}$ equal to -1.0, the passage geometry is square in the $\xi\theta$-plane and the average passage width in the $r\theta$-plane is approximately equal to the passage height (example III, fig. 6).

The parameter A is a function of $\frac{\ln r_h}{\Delta\theta}$ because passages with the same value of $\frac{\ln r_h}{\Delta\theta}$ have geometrically similar boundaries in the $\xi\theta$-plane, where the solution of equation (5), which solution determines A, is obtained. The right side of equation (5) indicates, however, that the solution of equation (5), and therefore the value of A, depends not only on the passage shape in the $\xi\theta$-plane, that is on $\frac{\ln r_h}{\Delta\theta}$, but also on the corresponding values of r at each value of ξ. Thus, the

value of A must also depend on the hub-tip radius ratio r_h. However, figure 11 shows that r_h has only a small effect on A for the range of r_h investigated.

For the range of α investigated by the numerical examples ($0 \leq \alpha \leq 1.0$), figure 10 shows that the variation in $(\beta - \beta_0)_1$ with α is similar for $0 \leq A \leq 0.3$ (also compare examples I, II, and IV in figs. 4(a), 5, and 7, respectively); and, if the curves of constant A are numbered in reverse order, figure 10 indicates the variation in $(\beta - \beta_0)_2$ with α is similar for $1.7 \leq A \leq 2.0$. In both cases the rotation of the central flow surfaces is similar for the specified range of A because for this range the corresponding values of $\frac{\ln r_h}{\Delta\theta}$ (fig. 11) are such that the passage walls parallel to the initial positions ($\alpha = 0$) of the central flow surfaces are too far removed to exert an important influence on the rotation $(\beta - \beta_0)$, which is therefore affected primarily by the angle α. It is therefore concluded that: (1) For values of $\frac{\ln r_h}{\Delta\theta}$ algebraically less than -2, the rotation of central S_1-surfaces is about the same for α less than 1.0; and (2) for values of $\frac{\ln r_h}{\Delta\theta}$ algebraically greater than -0.5, the rotation of central S_2-surfaces is about the same for α less than 1.0.

Distortion of flow surfaces. - Factors affecting the distortion of the flow surfaces are evident from figures 4 to 8. In general, a surface becomes distorted if (1) the fluid line that generates the surface approaches the vicinity of a corner in the $r\theta$-plane and (2) the center, or tangency point of the fluid line, moves closer to one of the passage boundaries. The relative importance of these factors depends on the particular passage geometry and the orientation of the flow surface. From figure 4(b), if the fluid line of the off-center flow surfaces is initially oriented ($\alpha = 0$) normal to the longer side of the passage boundary, the first factor is of major importance. From figure 4(c), if the fluid line of the off-center flow surfaces is initially oriented parallel to the longer side, the second factor is most important. For central flow surfaces, only the first factor exists.

It is clearly evident from figure 4(d) that for values of α considerably larger than 1.0 the flow surfaces become greatly distorted.

Effect of $\frac{\ln r_h}{\Delta\theta}$. - Table II and figure 11 indicate an approximate correlation of the parameter A with the ratio $\frac{\ln r_h}{\Delta\theta}$. Because A is an important parameter in the calculation of the rotation $(\beta - \beta_0)$ by

equation (7), this correlation suggests that $\frac{\ln r_h}{\Delta\theta}$ is an important parameter affecting the shape of the flow surfaces.

In table II the value of $\frac{\ln r_h}{\Delta\theta}$ is nearly the same for examples II and IV, and a comparison of these examples in figures 5 and 7 indicates great similarity in the shape of the flow surfaces. Also, in table II, $\frac{\ln r_h}{\Delta\theta}$ for example I and $\frac{\Delta\theta}{\ln r_h}$ for example V are of the same general order of magnitude. A comparison of the S_1- and S_2-surfaces of example I in figure 4(a) with the S_2- and S_1-surfaces, respectively, of example V in figure 8 indicates considerable similarity. It is therefore concluded that, for the same value of $\frac{\ln r_h}{\Delta\theta}$, or its inverse, axial-flow passages of the type investigated have similar shapes of flow surfaces.

SUMMARY OF RESULTS AND CONCLUSIONS

Three-dimensional, incompressible, nonviscous, absolute irrotational fluid motion is investigated for flow through rotating axial-flow passages bounded by straight blades of finite spacing and infinite axial length lying on meridional planes. Solutions are obtained for five passage geometries described by various ratios of the logarithm of the hub-tip ratio divided by the blade spacing $\frac{\ln r_h}{\Delta\theta}$, and the results are presented in such a manner as to apply for all ratios of axial velocity to passage tip speed.

The solutions are used to determine the deviation of flow surfaces from their assumed orientation in the usual type of two-dimensional solution. This deviation is shown by the fluid-line positions (intersections of the flow surfaces with the $r\theta$-plane) for equal increments of the angle α that the passage rotates about the z-axis as the flow surface deviates from its initial orientation. The deviation is considered to consist in (1) displacement in the $r\theta$-plane of the center point of the fluid line, (2) rotation in the $r\theta$-plane of the fluid line about its center point, and (3) distortion of the fluid line in the $r\theta$-plane.

Two types of flow surface are considered: S_1- and S_2-surfaces initially oriented along circumferential and radial lines, respectively, in the $r\theta$-plane. The surfaces are central flow surfaces if they pass through the point of zero relative velocity at the passage center in the $r\theta$-plane; otherwise, the surfaces are off-center flow surfaces.

Some results of the numerical examples are:

1. The central flow surfaces rotate relative to the passage about a straight axial line through the point of minimum stream function near the center of the passage in the $r\theta$-plane.

2. For any off-center flow surface the envelope of the fluid-line positions in the $r\theta$-plane for various values of α is a streamline.

Some conclusions resulting from the numerical examples are:

1. For values of α corresponding to conditions in typical axial-flow blade rows, the deviation of flow surfaces is not large.

2. For values of α less than 1.0 radian, the rotation of the central S_1-surface is about the same in all passages for which $\frac{\ln r_h}{\Delta\theta}$ is algebraically less than -2.0.

3. For values of α less than 1.0 radian, the rotation of the central S_2-surface is about the same in all passages for which $\frac{\ln r_h}{\Delta\theta}$ is algebraically greater than -0.5.

4. In general, a flow surface becomes distorted if (a) the fluid line that generates the surface approaches the vicinity of a corner in the $r\theta$-plane and (b) the center point of the fluid line moves closer to one of the passage boundaries.

5. For values of α considerably greater than 1.0 radian, the flow surfaces become greatly distorted.

6. For the same value of $\frac{\ln r_h}{\Delta\theta}$, axial-flow passages of the type investigated have similar shapes of flow surfaces.

Lewis Flight Propulsion Laboratory
National Advisory Committee for Aeronautics
Cleveland, Ohio, August 1, 1952

APPENDIX A

SYMBOLS

The following symbols are used in this report. All symbols are dimensionless, unless otherwise specified. Velocities are expressed as ratios of the passage-tip speed; distances are expressed as ratios of the passage-tip radius.

A parameter, which is the value of $\frac{\partial^2\psi}{\partial r^2}$ at the center point ($\psi^* = 1.0$) about which the central flow surfaces rotate, equation (B3a) of appendix B

r,θ,z cylindrical coordinates relative to rotating passage (fig. 1)

S flow surface generated by motion through passage of any fluid line consisting of the same fluid particles and extending from one boundary to another in $r\theta$-plane

s arc length along flow surface in $r\theta$-plane

u,v,w relative velocity components in r, θ, z directions, respectively, (fig. 1)

α absolute angle that passage has rotated about z-axis from initial position at which fluid lines for S_1- and S_2-surfaces are circumferential and radial lines, respectively, in $r\theta$-plane

β angle of tangent to fluid line at its center point in $r\theta$-plane, measured clockwise from radial direction

$\Delta\theta$ blade spacing in $r\theta$-plane

ξ transformed coordinate, equation (4)

ψ stream function in $r\theta$-plane, equation (2)

ψ^* stream function ψ divided by ψ_{min}, equation (7)

Ω relative angular velocity of elemental arc ds, of central flow surface, rotating about point $\psi^* = 1.0$ in $r\theta$-plane, expressed as ratio of ω'

ω' absolute angular velocity of passage about z-axis, dimensional

Subscripts:

h hub (so that r_h is hub-tip ratio)

min minimum

0 initial position, when α equals zero

1 flow surface with circumferential line for initial position of fluid line in $r\theta$-plane

2 flow surface with radial line for initial position of fluid line in $r\theta$-plane

Superscript:

' dimensional quantities

APPENDIX B

ROTATION OF CENTRAL S_1- AND S_2-SURFACES ABOUT THEIR CENTER POINT IN $r\theta$-PLANE

If Ω is the relative angular velocity, expressed as a ratio of the absolute angular velocity of the passage about the z-axis, of an elemental arc length ds rotating about the point $\psi^* = 1.0$ in the $r\theta$-plane, then from figure 12

$$\Omega \, ds = \frac{\partial v}{\partial s} ds \cos \beta - \frac{\partial u}{\partial s} ds \sin \beta \tag{B1}$$

where

$$\frac{\partial v}{\partial s} = \frac{\partial v}{\partial r}\frac{dr}{ds} + \frac{\partial v}{\partial \theta}\frac{d\theta}{ds} = \frac{\partial v}{\partial r} \cos \beta + \frac{1}{r}\frac{\partial v}{\partial \theta} \sin \beta \tag{B1a}$$

and

$$\frac{\partial u}{\partial s} = \frac{\partial u}{\partial r} \cos \beta + \frac{1}{r}\frac{\partial u}{\partial \theta} \sin \beta \tag{B1b}$$

At the point for $\psi^* = 1.0$, however, u and v are equal to zero and, because the streamlines are normal to the passage center line,

$$\frac{\partial u}{\partial r} = 0 \tag{B2a}$$

so that the continuity equation (1) gives

$$\frac{\partial v}{\partial \theta} = 0 \tag{B2b}$$

and equation (3a) becomes

$$\frac{1}{r}\frac{\partial u}{\partial \theta} = 2 + \frac{\partial v}{\partial r} \tag{B2c}$$

From equations (B1) and (B2)

$$\Omega = \frac{\partial v}{\partial r} (\cos^2 \beta - \sin^2 \beta) - 2 \sin^2 \beta$$

or, from equation (2b),

$$-\Omega = A + 2(1 - A) \sin^2 \beta \tag{B3}$$

where

$$A = \frac{\partial^2 \psi}{\partial r^2} \tag{B3a}$$

Also, it can be shown from the definition of Ω that

$$\Omega = \frac{d\beta}{d\alpha}$$

so that, from equation (B3),

$$\alpha = -\int_{\beta_0}^{\beta} \frac{d\beta}{A + 2(1 - A)\sin^2\beta}$$

or

$$\alpha = \frac{1}{\sqrt{A(2 - A)}}\left[\tan^{-1}\left(\sqrt{\frac{2 - A}{A}}\tan\beta_0\right) - \tan^{-1}\left(\sqrt{\frac{2 - A}{A}}\tan\beta\right)\right] \tag{B4}$$

For central S_1-surfaces, β_0 equals 90° so that

$$\tan\beta_1 = \sqrt{\frac{A}{2 - A}}\tan\left[\frac{\pi}{2} - \alpha\sqrt{A(2 - A)}\right]$$

and

$$\tan(\beta - \beta_0)_1 = -\sqrt{\frac{2 - A}{A}}\tan\left[\alpha\sqrt{A(2 - A)}\right] \tag{7a}$$

For central S_2-surfaces, β_0 equals 0 so that

$$\tan\beta_2 = \sqrt{\frac{A}{2 - A}}\tan\left[-\alpha\sqrt{A(2 - A)}\right]$$

and

$$\tan(\beta - \beta_0)_2 = -\sqrt{\frac{A}{2 - A}}\tan\left[\alpha\sqrt{A(2 - A)}\right] \tag{7b}$$

REFERENCES

1. Stanitz, John D., and Ellis, Gaylord O.: Two-Dimensional Flow on General Surfaces of Revolution in Turbomachines. NACA TN 2654, 1952.

2. Wu, Chung-Hua, and Brown, Curtis A.: Method of Analysis for Compressible Flow Past Arbitrary Turbomachine Blades on General Surface of Revolution. NACA TN 2407, 1951.

3. Ellis, Gaylord O., Stanitz, John D., and Sheldrake, Leonard J.: Two Axial-Symmetry Solutions for Incompressible Flow Through a Centrifugal Compressor with and without Inducer Vanes. NACA TN 2464, 1951.

4. Hamrick, Joseph T., Ginsburg, Ambrose, and Osborn, Walter M.: Method of Analysis for Compressible Flow Through Mixed-Flow Centrifugal Impellers of Arbitrary Design. NACA TN 2165, 1950.

5. Wu, Chung-Hua: A General Theory of Three-Dimensional Flow in Subsonic and Supersonic Turbomachines of Axial-, Radial-, and Mixed-Flow Types. NACA TN 2604, 1952.

6. Southwell, R. V.: Relaxation Methods in Theoretical Physics. Clarendon Press (Oxford), 1946.

7. Emmons, Howard W.: The Numerical Solution of Compressible Fluid Flow Problems. NACA TN 932, 1944.

8. Ellis, Gaylord O., and Stanitz, John D.: Comparison of Two- and Three-Dimensional Potential-Flow Solutions in a Rotating Impeller Passage. NACA TN 2806, 1952.

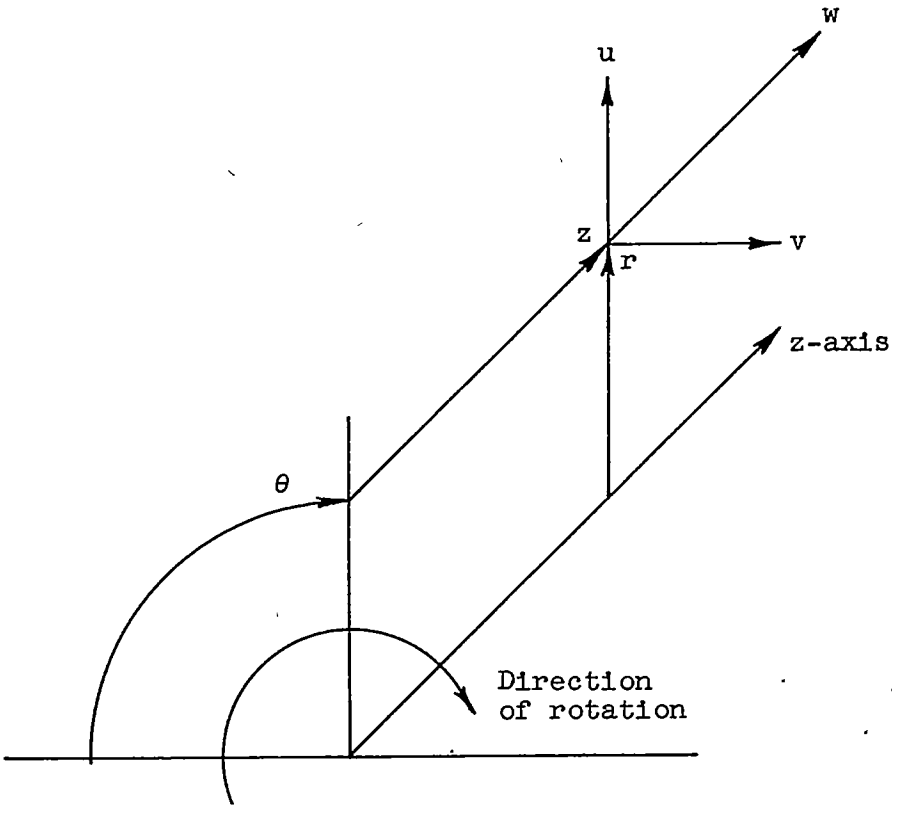

Figure 1. - Cylindrical coordinates and velocity components relative to rotating passage.

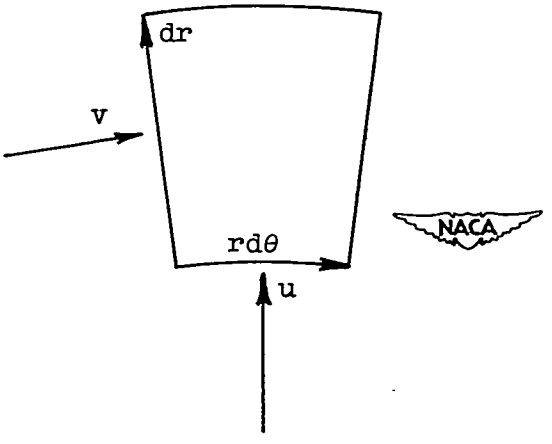

Figure 2. - Fluid particle in rθ-plane.

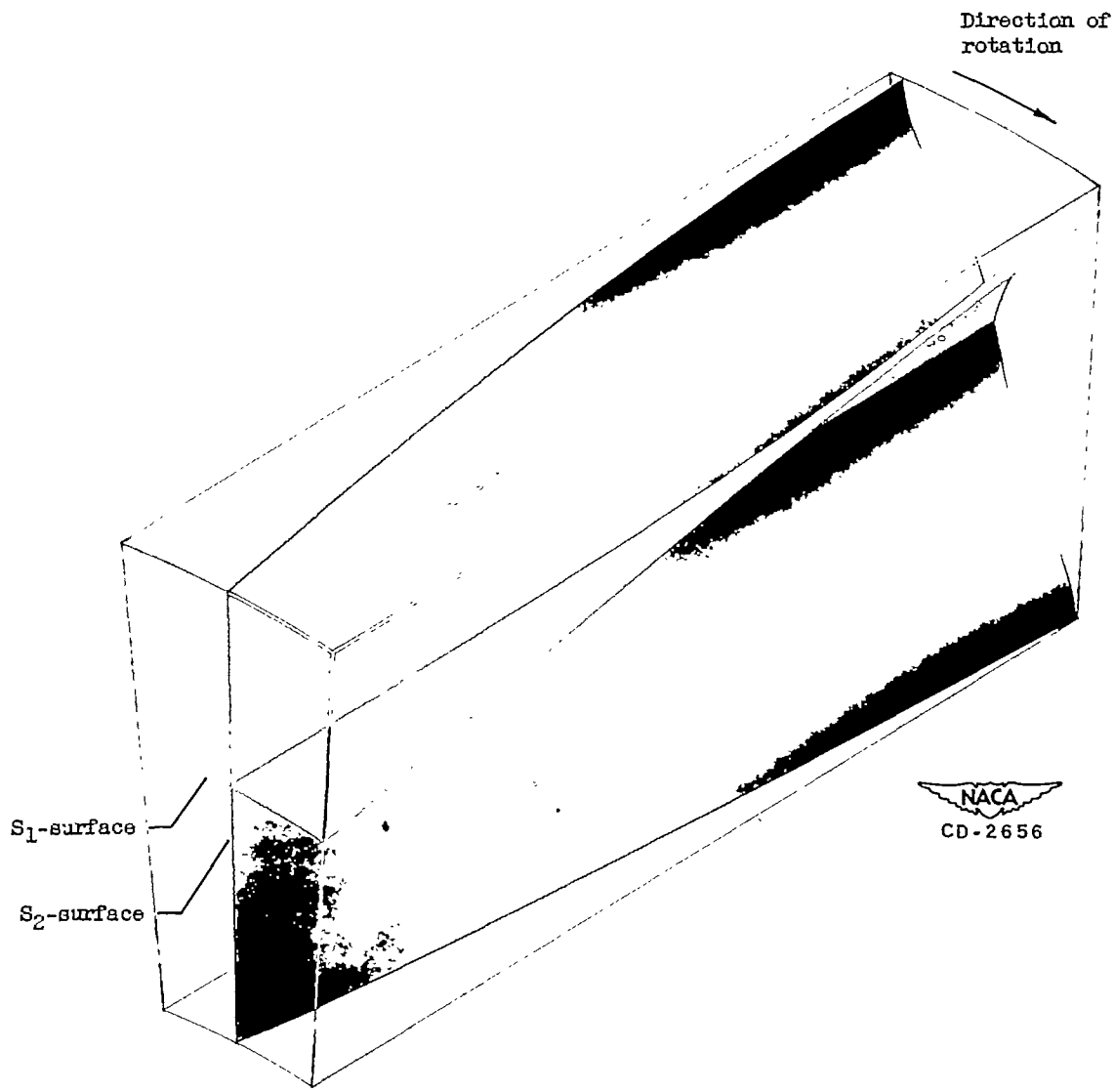

Figure 3. - Central S_1- and S_2-surfaces for example I with axial velocity w equal to 0.6.

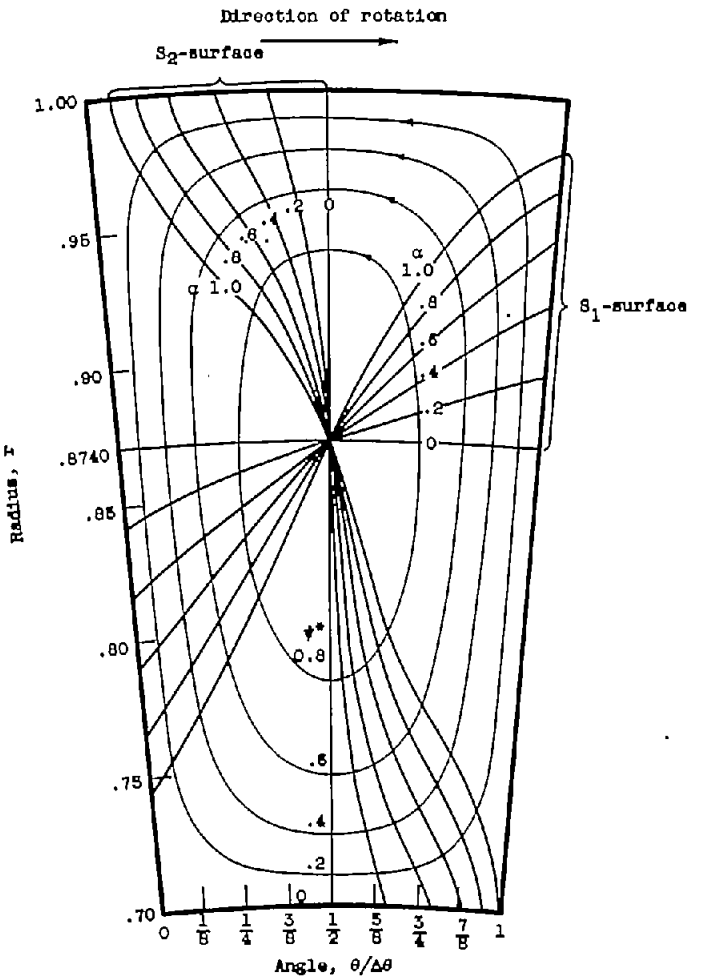

(a) Central S_1- and S_2-surfaces.

Figure 4. - Fluid-line positions of flow surfaces for example I. Hub-tip ratio, r_h, 0.7000; blade spacing, $\Delta\theta$, $10^{\circ}13'$; minimum value of ψ, -0.00524.

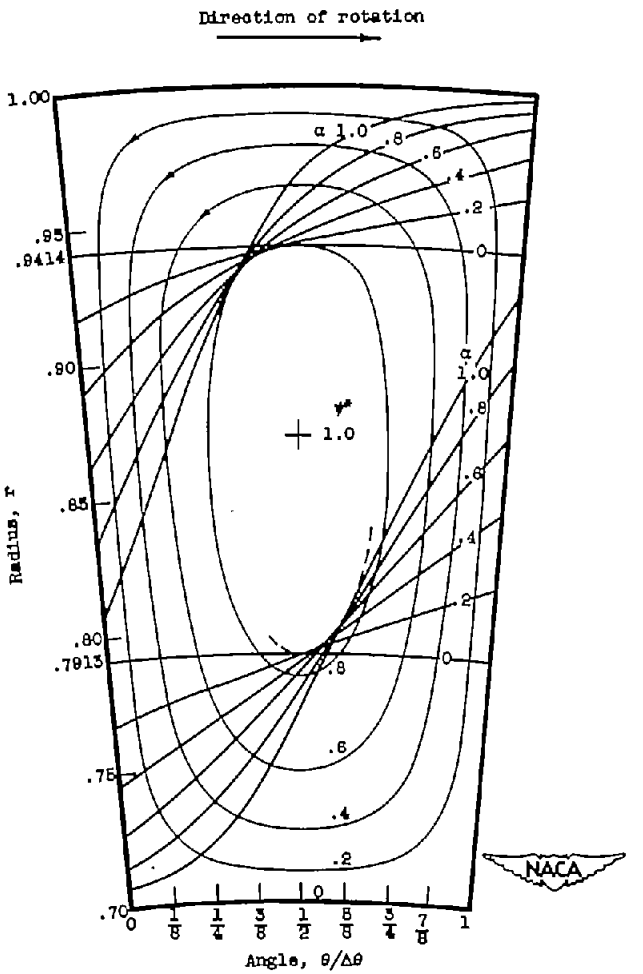

(b) Off-center S_1-surfaces.

Figure 4. - Continued. Fluid-line positions of flow surfaces for example I. Hub-tip ratio, r_h, 0.7000; blade spacing, $\Delta\theta$, $10^{\circ}13'$; minimum value of ψ, -0.00524.

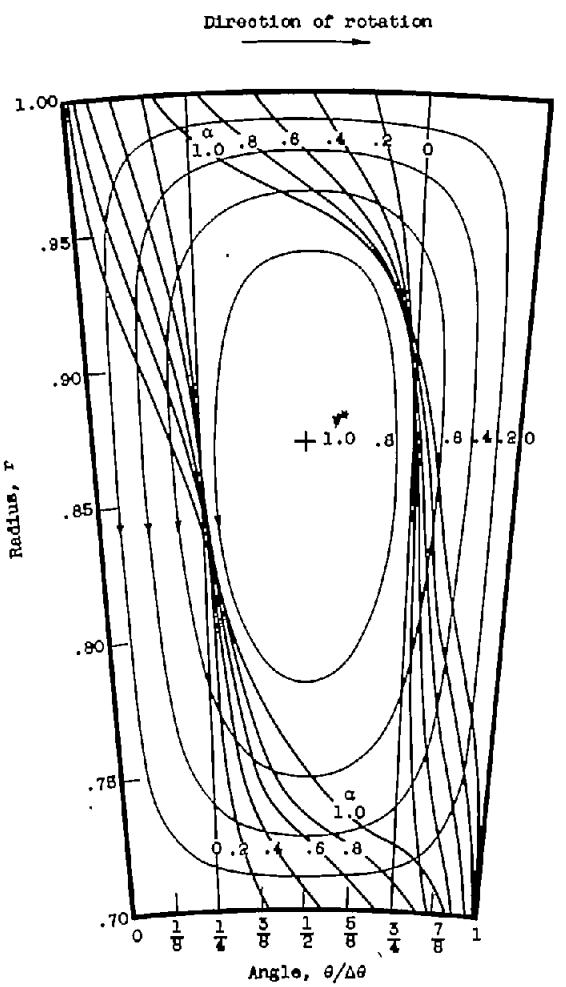

(c) Off-center S_2-surfaces.

Figure 4. - Continued. Fluid-line positions of flow surfaces for example I. Hub-tip ratio, r_h, 0.7000; blade spacing, $\Delta\theta$, 10°13'; minimum value of ψ, -0.00524.

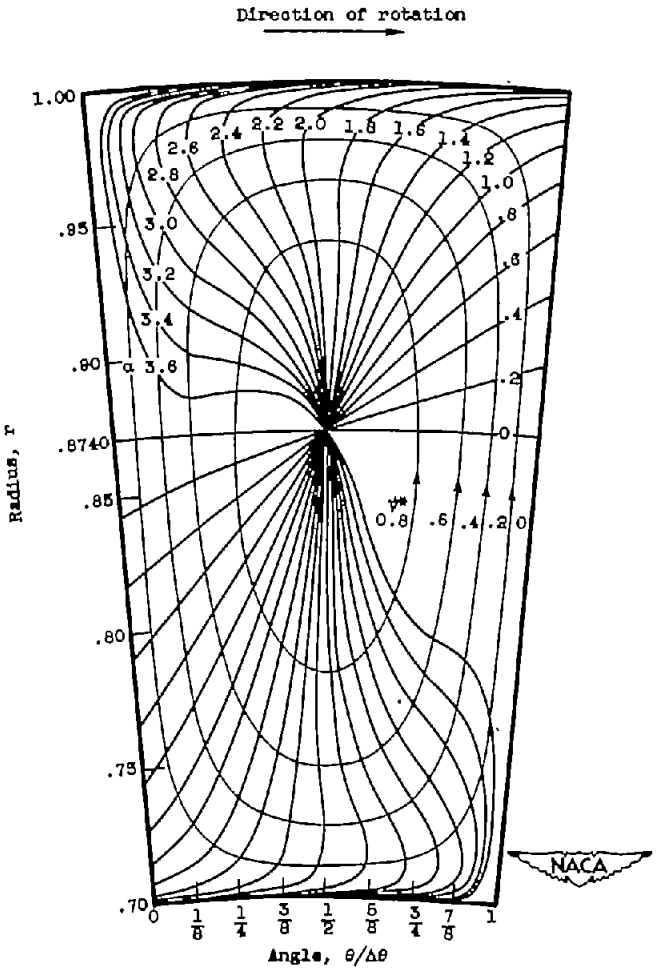

(d) Distortion of central S_1-surface for wide range of α.

Figure 4. - Concluded. Fluid-line positions of flow surfaces for example I. Hub-tip ratio, r_h, 0.7000; blade spacing, $\Delta\theta$, 10°13'; minimum value of ψ, -0.00524.

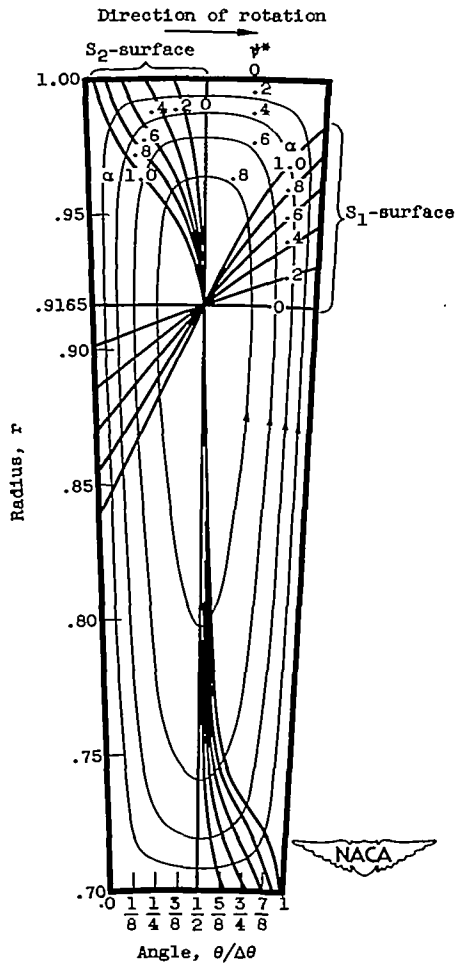

Figure 5. - Fluid-line positions of central S_1- and S_2-surfaces for example II. Hub-tip ratio, r_h, 0.7000; blade spacing, $\Delta\theta$, $5^{\circ}7'$; minimum value of ψ, -0.00157.

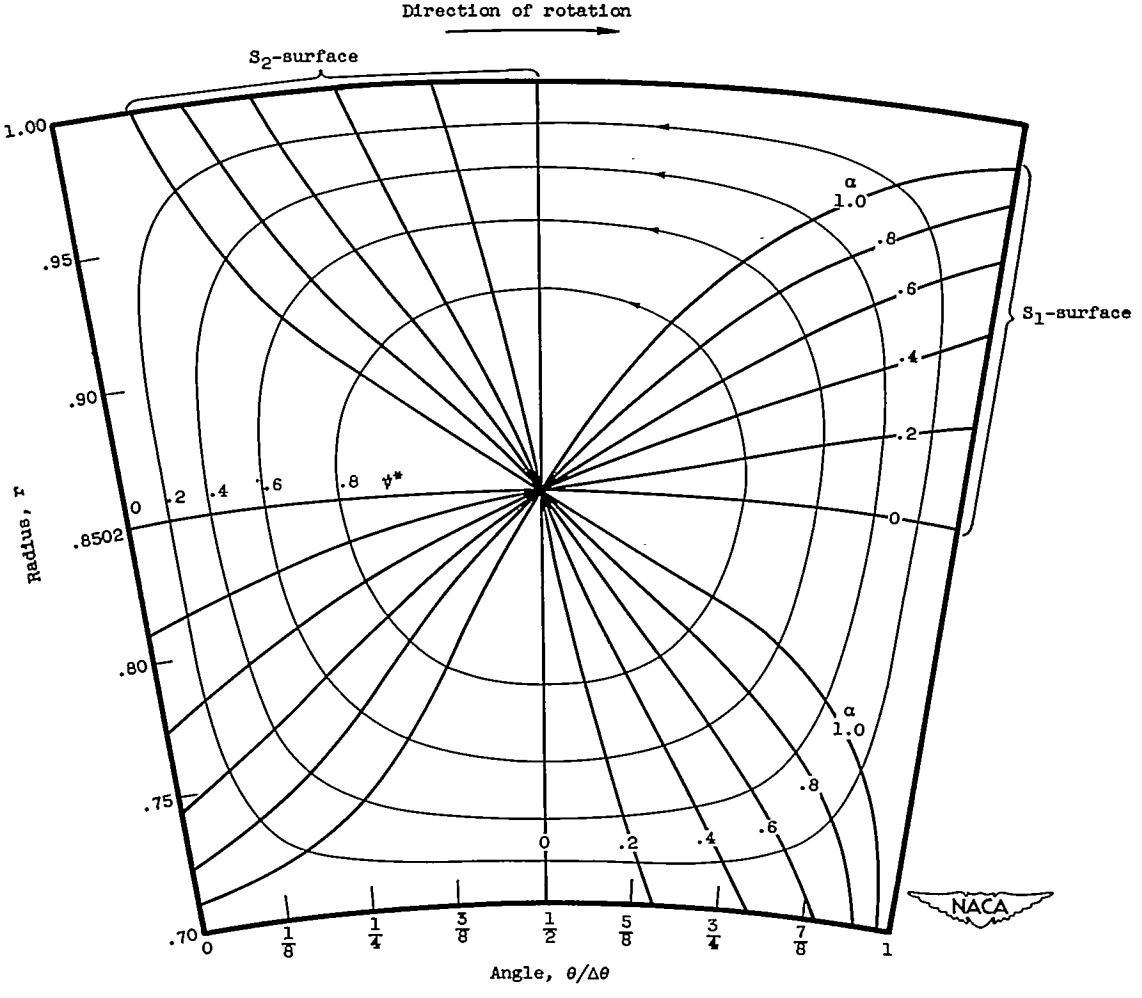

Figure 6. - Fluid-line positions of central S_1- and S_2-surfaces for example III. Hub-tip ratio, r_h, 0.7000; blade spacing, $\Delta\theta$, 20°26'; minimum value of ψ, -0.01318.

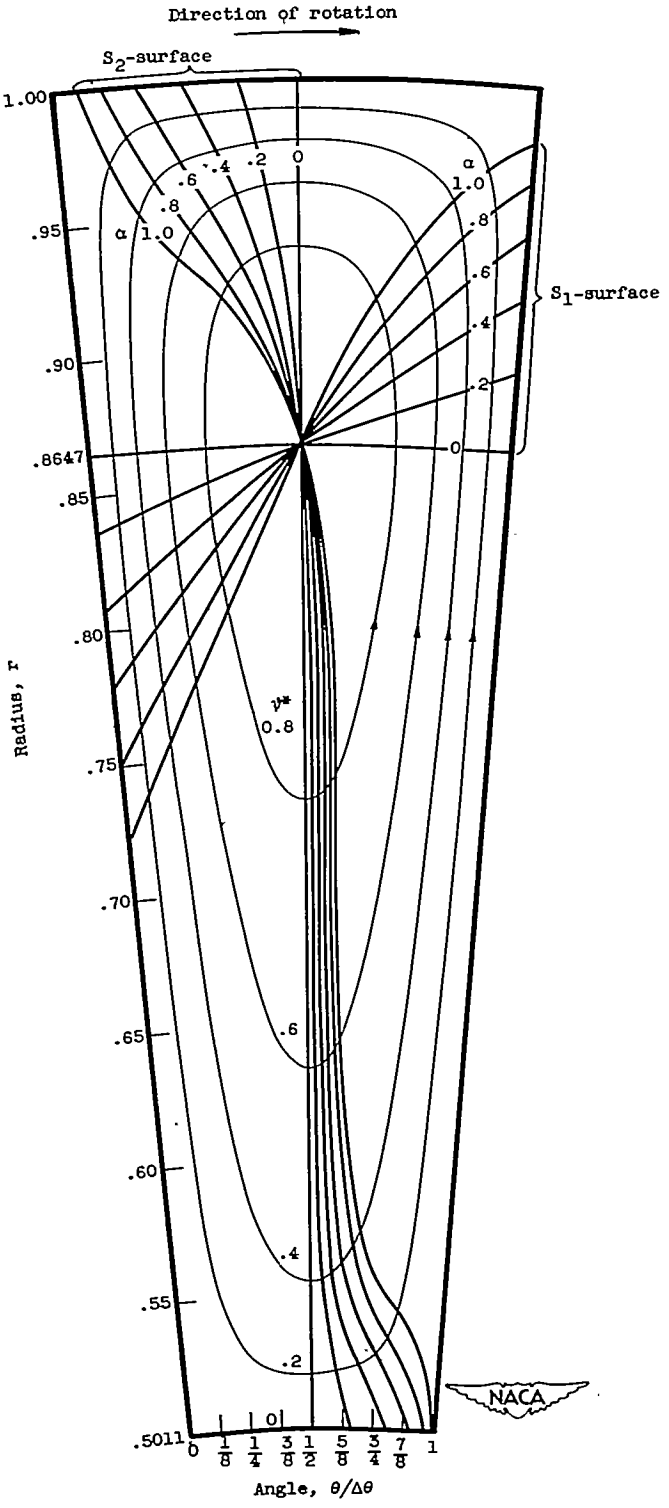

Figure 7. - Fluid-line positions of central S_1- and S_2-surfaces for example IV. Hub-tip ratio, r_h, 0.50105; blade spacing, $\Delta\theta$, $10^{\circ}13'$; minimum value of ψ, -0.00544.

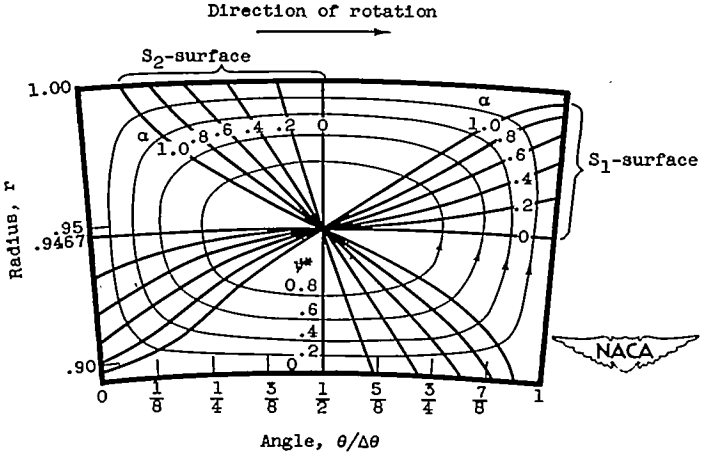

Figure 8. - Fluid-line positions of central S_1- and S_2-surfaces for example V. Hub-tip ratio, r_h, 0.89453; blade spacing, $\Delta\theta$, $10^{\circ}13'$; minimum value of ψ, -0.00231.

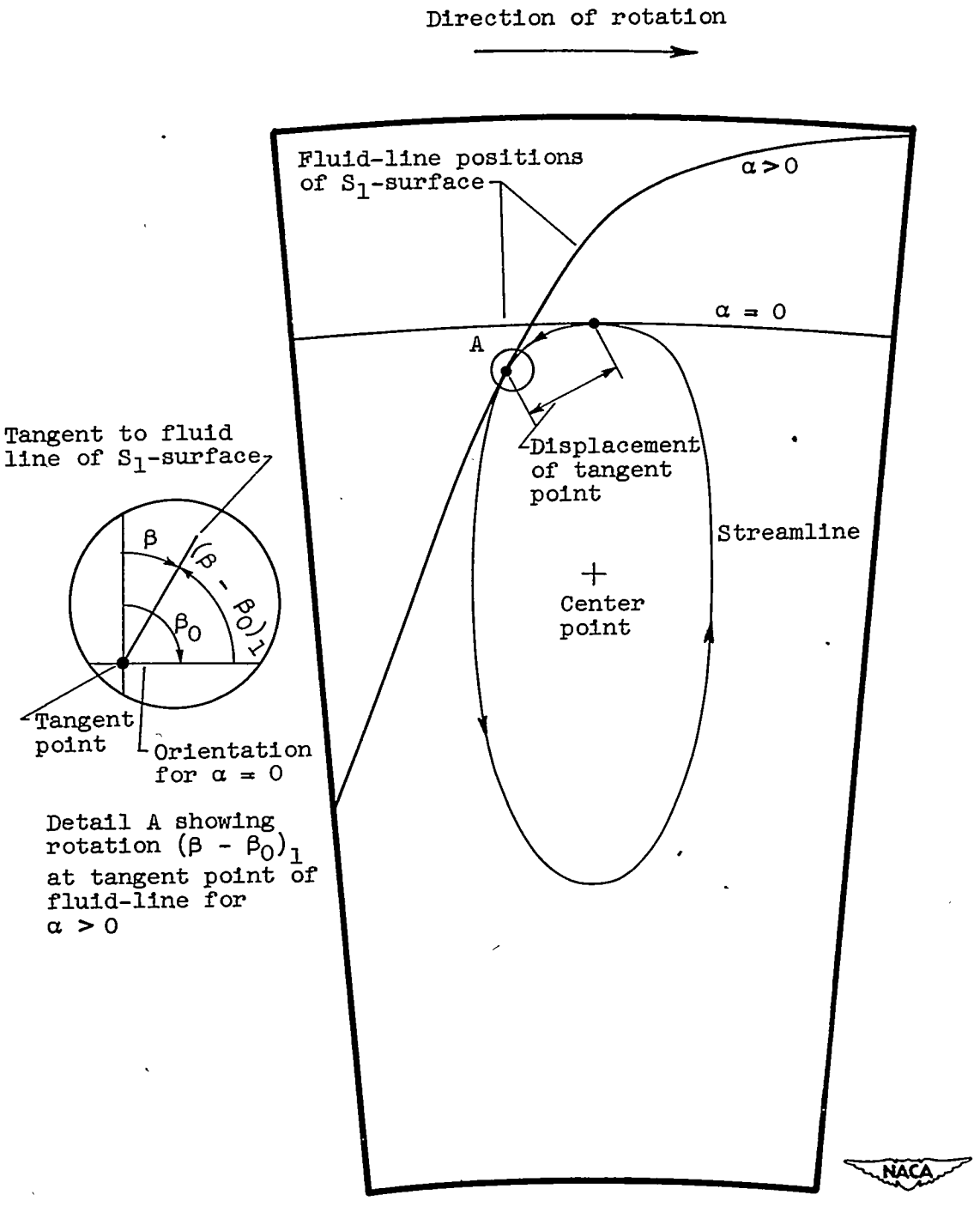

Figure 9. - Definitions of terms used to describe deviation of flow surfaces from initial orientation in $r\theta$-plane at $\alpha = 1.0$.

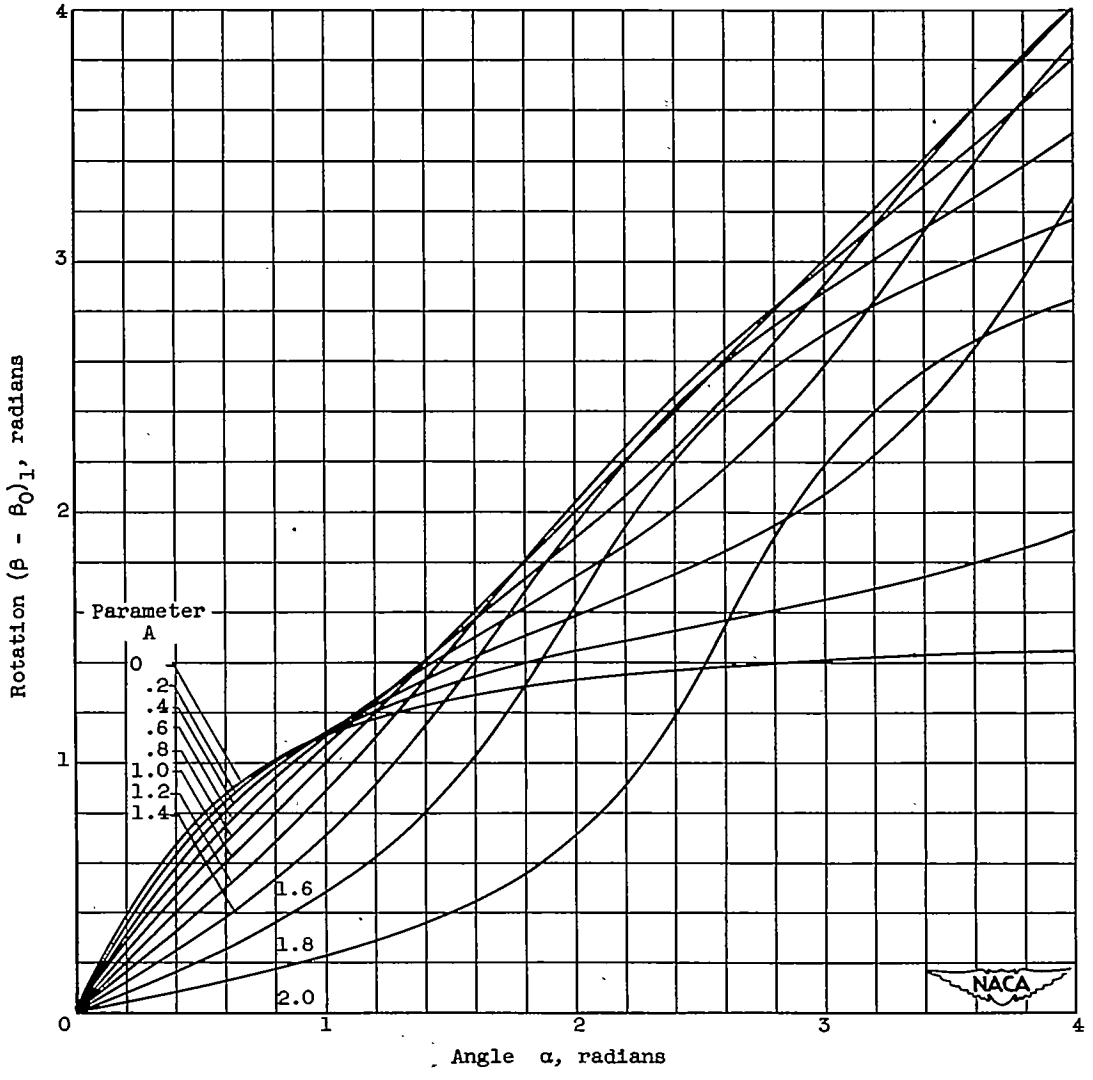

Figure 10. - Variation in rotation $(\beta - \beta_0)_1$ of central S_1-surfaces with angle α. Equation (7a).

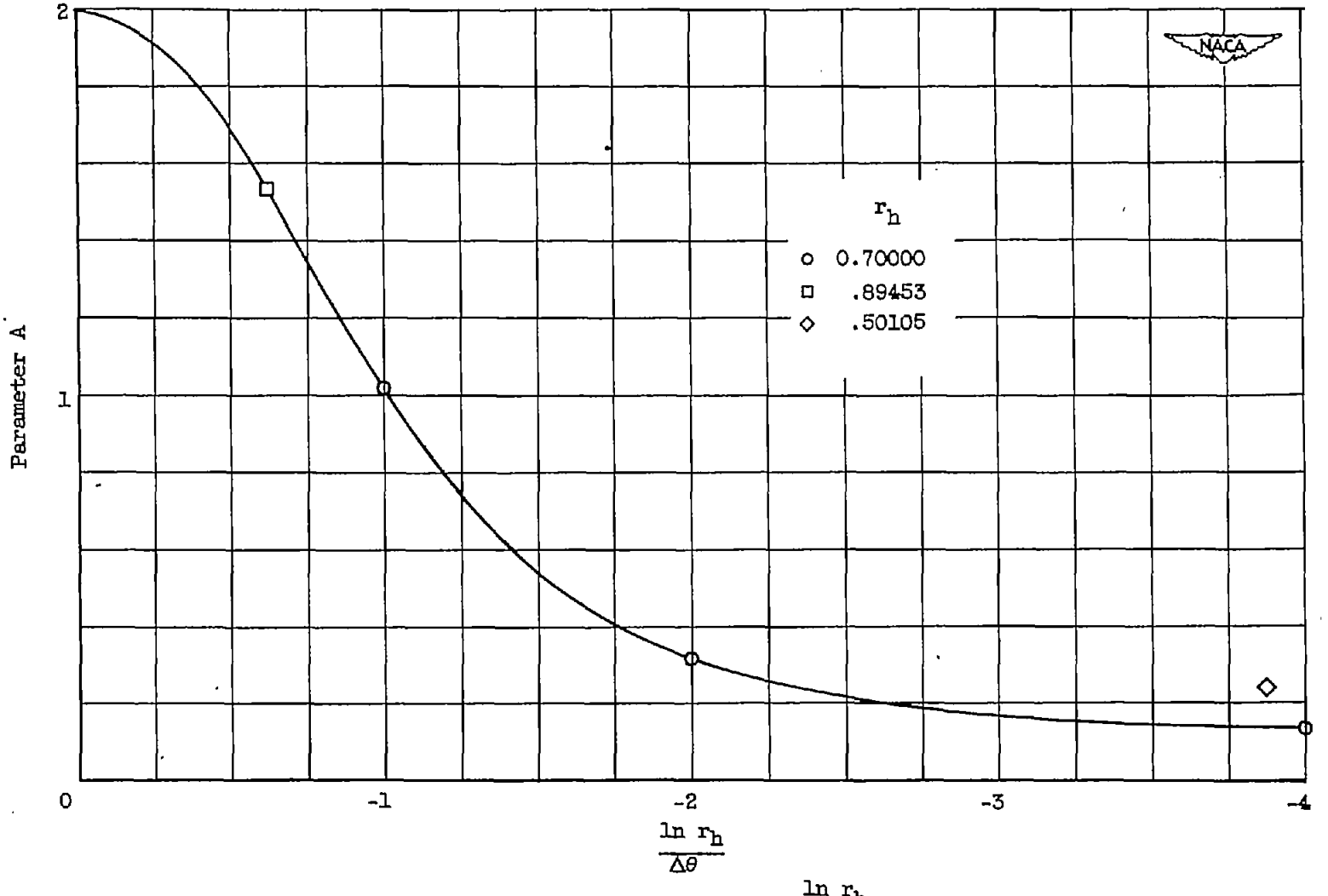

Figure 11. - Variation in parameter A with $\frac{\ln r_h}{\Delta\theta}$ for examples I to V.

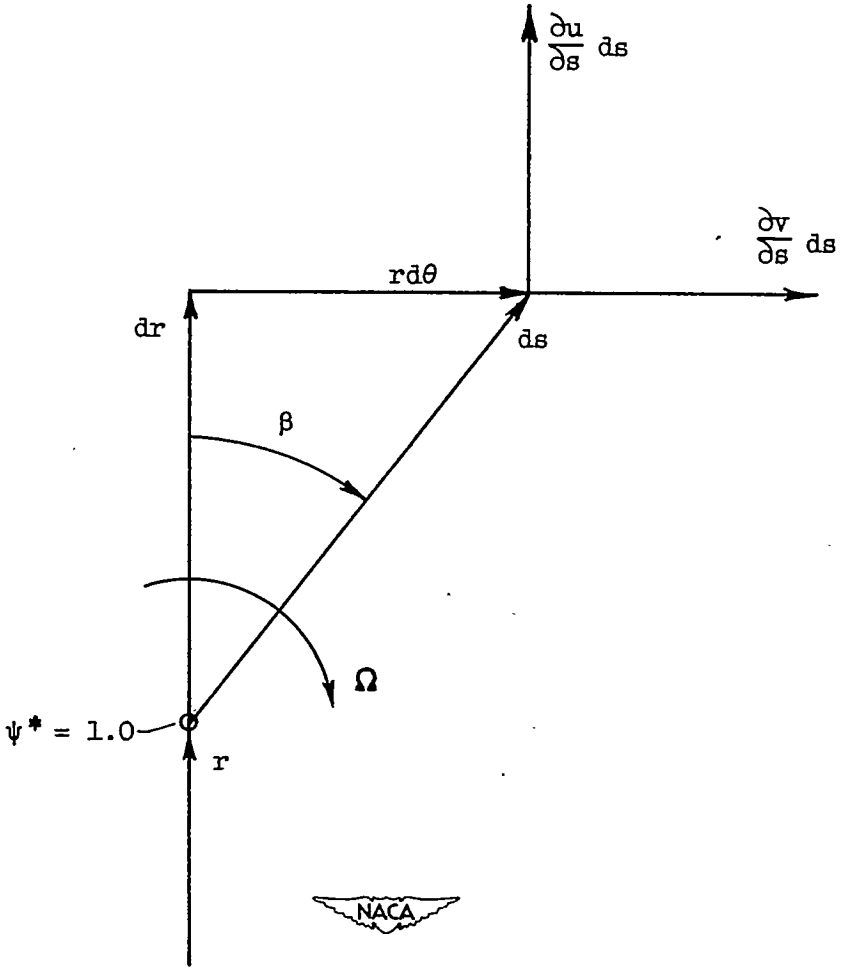

Figure 12. - Elemental arc ds of a fluid line rotating about point at which stream function $\psi^* = 1.0$ in $r\theta$-plane.

NACA-Langley - 11-18-52 -1000